JPET Fast Forward. Published on July 12, 2018 as DOI: 10.1124/jpet.118.250134
This article has not been copyedited and formatted. The final version may differ from this version.

JPET#250134

Role of interstitial fluid turnover on target suppression by therapeutic biologics using a minimal physiologically-based pharmacokinetic (mPBPK) model

Xiaobing Li, William J. Jusko, and Yanguang Cao

Department of Pharmacy, Shengjing Hospital of China Medical University, Shenyang, China (X.L.); Division of Pharmacotherapy and Experimental Therapeutics, UNC Eshelman School of Pharmacy, University of North Carolina at Chapel Hill, Chapel Hill (X.L., Y.C.); and Department of Pharmaceutical Sciences, School of Pharmacy and Pharmaceutical, Sciences, State University of New York at Buffalo, Buffalo, New York (W.J.J.)

Running Title: ISF Turnover Affects Target Suppression of Therapeutic Biologics

Corresponding Author: Yanguang Cao, Division of Pharmacotherapy and Experimental Therapeutics, 2318 Kerr Hall, UNC Eshelman School of Pharmacy, University of North Carolina at Chapel Hill, Chapel Hill, NC 27599-7569.

Phone: +1-919-966-4040. Fax: +1-919-962-0644. E-mail: yanguang@unc.edu

Number of text pages: 35

Number of tables: 2

Number of Figures: 5

Number of references: 62

Number of words in Abstract: 224

Number of words in Introduction: 677

Number of words in Discussion: 920

ABBREVIATIONS: ISF, interstitial fluid; mAbs, monoclonal antibodies; mPBPK, minimal physiologically-based pharmacokinetic model; TMDD, target-mediated drug disposition; TNF-α, tumor necrosis factor-α.

JPET Fast Forward. Published on July 12, 2018 as DOI: 10.1124/jpet.118.250134
This article has not been copyedited and formatted. The final version may differ from this version.

Abstract

For therapeutic biologics against soluble ligands, the magnitude and duration of target suppression affects their therapeutic efficacy. Many factors have been evaluated in relation to target suppression but interstitial fluid turnover rate in target tissues has not been considered. Inspired by the fact that etanercept exerts limited efficacy for Crohn's Disease despite its high efficacy for Rheumatoid Arthritis, we developed a minimal PBPK model to investigate the role of tissue fluid turnover rate on soluble target suppression and assessed the interrelationships between binding constants and tissue fluid turnover. Interstitial fluid turnover rates in target tissues were found to strongly influence target binding kinetics. For tissues with low fluid turnover, stable binders (low k_{off}) exhibit greater target suppression, but efficacy is often restricted by accumulation of drug-target complex. For tissues with high fluid turnover, fast binders (high k_{on}) are generally favored but a plateau effect is present for antibodies with low dissociation rates (k_{off}). Etanercept is often regarded as a fast TNF-α binder (high k_{on}) despite comparable binding affinity (K_D, k_{off}/k_{on}) with adalimumab and infliximab. Crohn's Disease largely involves the colon, a tissue with relatively slower fluid turnover than arthritis-associated joint synovium; this may explain why etanercept exerts poor TNF-α suppressive effect for Crohn's Disease. This study highlights the importance of tissue interstitial fluid turnover in evaluation of therapeutic antibodies bound to soluble antigens.

Introduction

Several therapeutic biologics that neutralize or block a soluble pro-inflammatory cytokine TNF-α have demonstrated strong efficacy in treatment of autoimmune diseases, such as Rheumatoid Arthritis (RA) and Crohn's Disease (CD) (Feldmann et al., 1996; Pizarro and Cominelli, 2007; van Schouwenburg et al., 2013). Monoclonal antibodies (mAbs) like adalimumab and infliximab, and a fusion protein etanercept all exhibit high specificity and affinity for binding to soluble TNF-α and display therapeutic efficacy for RA (Garrison and McDonnell, 1999; Markham and Lamb, 2000; Bang and Keating, 2004). Surprisingly, when using these biologics for CD, another autoimmune disease for which TNF-α is a critical pathogenic factor, only adalimumab and infliximab but not etanercept show sufficient efficacy (Olesen et al., 2016). The reason for this difference have focused on the distinct binding affinities of these biologics to trans-membrane TNF-α and the role of trans-membrane TNF-α in the pathogenesis of CD (Tracey et al., 2008; Horiuchi et al., 2010). Unfortunately, it remains unclear why there is limited efficacy of etanercept in treatment of CD.

For therapeutic biologics that bind to soluble ligands, their efficacy is largely determined by the magnitude and duration of ligand suppression (Wang et al., 2008). According to previous reports (Kim et al., 2007; Song et al., 2008), adalimumab and infliximab have relatively slower association and dissociation rates than etanercept when binding to soluble TNF-α, even though all biologics exhibit comparable binding affinities (K_D) in the sub-nM range. In addition, compared with etanercept, infliximab and adalimumab frequently form large immune complexes once bound to one or more trimers of soluble TNF-α (Scallon et al., 2002). Such large immune complexes may be

responsible for their high risk of tuberculosis (Fallahi-Sichani et al., 2012). For etanercept, such large immune complexes have seldomly been reported and the risk of tuberculosis is relatively low (Cantini et al., 2014). There is similar efficacy among the three biologics for RA (Aaltonen et al., 2012). It remains a puzzle why etanercept lacks sufficient efficacy for CD whereas the other two biologics exhibit strong effect. Here a modeling approach was used to explore the underlying mechanisms, particularly focusing on differences in TNF-α binding kinetics and role of interstitial fluid turnover.

For many antibody-based biologics, the interstitial space within the diseased tissues is their actual sites of action. Tissue interstitial fluid (ISF) is generally believed to be the major extravascular distribution space for antibody-based biologics (Cao et al., 2013; Eigenmann et al., 2017). Vascular convection drives antibody distribution into ISF and then lymphatic drainage provides removal from tissue ISF back into the circulation. The efficiency of lymphatic drainage in target tissues, which essentially determines ISF turnover rate, is expected to affect antibody-target binding kinetics and binding equilibrium, and might further influence the magnitude and duration of target suppression (Guo et al., 2009; Zhou et al., 2011; Becker et al., 2015). The ISF turnover varies greatly among tissues. For antibodies bound to soluble antigens, evaluating the influence of tissue ISF turnover on target suppression and therapeutic efficacy in disease-associated tissues is warranted.

The second-generation minimal physiologically based pharmacokinetic (mPBPK) model accommodates the fundamental distribution mechanisms of mAbs or fusion proteins, such as lymphatic convection and drainage, and ISF as the primary extravascular distribution space (Cao et al., 2013; Cao and Jusko, 2014b). This modeling

approach provides a reasonable approximation of antibody concentrations in interstitial fluid, and allows incorporating antibody-target binding kinetics in plasma and/or tissue interstitium, or any other disease-associated tissues (Cao and Jusko, 2014a; Chen et al., 2016; Chen et al., 2017). The present assessment extends the original mPBPK model with a specific disease-associated tissue, where a dynamic interstitial fluid turnover was defined. The impact of tissue ISF turnover on TNF-α suppression among three TNF-α antagonists (etanercept, adalimumab, and infliximab) was evaluated to test whether the differences of tissue ISF turnover would explain the limited efficacy of etanercept in CD. Antigen binding kinetics in target tissues for biologics with soluble targets was also explored to test the influence of tissue fluid turnover on target binding kinetics and target suppression. This concept was applied to survey 27 licensed antibodies that bind to soluble ligands for various indications, and evaluated how fluid turnover of their target tissues influenced their efficacy.

JPET Fast Forward. Published on July 12, 2018 as DOI: 10.1124/jpet.118.250134
This article has not been copyedited and formatted. The final version may differ from this version.

Materials and Methods

An extended minimal PBPK model

As shown in **Fig. 1**, a second-generation mPBPK model is proposed with a specific disease-associated tissue compartment to assess the impact of tissue ISF turnover on the therapeutic efficacy of biologics that bind to soluble antigens. The mPBPK model is described by the equations:

$$\frac{dC_p}{dt} = \frac{L \cdot C_{lymph} - L_1 \cdot (1-\sigma_1) \cdot C_p - L_2 \cdot (1-\sigma_2) \cdot C_p - C_p \cdot CL_p}{V_p}$$

$$C_p\,(0) = 1000 \text{ nM} \quad (1)$$

$$\frac{dC_{tight}}{dt} = \frac{L_1 \cdot (1-\sigma_1) \cdot C_p - L_1 \cdot (1-\sigma_L) \cdot C_{tight}}{V_{tight}} \quad (2)$$

$$\frac{dC_{leaky}}{dt} = \frac{L_2 \cdot (1-\sigma_2) \cdot C_p - L_2 \cdot (1-\sigma_L) \cdot C_{leaky}}{V_{leaky}} \quad (3)$$

$$\frac{dC_{lymph}}{dt} = \frac{L_1 \cdot (1-\sigma_L) \cdot C_{tight} + L_2 \cdot (1-\sigma_L) \cdot C_{leaky} - L \cdot C_{Lymph}}{V_{lymph}} \quad (4)$$

where C_p and C_{lymph} are mAb concentrations in V_p (plasma volume) and V_{lymph} (lymph volume) in a 70 kg man, C_{tight} and C_{leaky} are mAb ISF concentrations in two groups of lumped tissues categorized by continuous and fenestrated vascular endothelium structures. There are V_{tight} ($0.65 \cdot ISF \cdot K_p$, where ISF is total system interstitial fluid and K_p is the available fraction of ISF for distribution) and V_{leaky} ($0.35 \cdot ISF \cdot K_p$) indicating ISF volumes for tight tissue (muscle, skin, adipose and brain) and leaky tissue (all other tissues like liver, kidney, heart, etc.) (Cao et al., 2013). The L is total lymph flow, equal the sum of L_1 (lymph flow for V_{tight}) and L_2 (lymph flow for V_{leaky}), where $L_1 = 0.33 \cdot L$ and $L_2 = 0.67 \cdot L$

JPET Fast Forward. Published on July 12, 2018 as DOI: 10.1124/jpet.118.250134
This article has not been copyedited and formatted. The final version may differ from this version.

(Shah and Betts, 2012). The σ_1 and σ_2 are vascular reflection coefficients for V_{tight} and V_{leaky}, and fixed to 0.95 and 0.71 (Cao and Jusko, 2014b). The σ_L is lymphatic reflection coefficient, assumed as 0.2 in this model (Garg and Balthasar, 2007). The CL_p is systemic clearance from plasma (Cao and Jusko, 2014b). All Initial Conditions = 0 except C_p = 1000 nM. In this model, the physiologic parameters (Davies and Morris, 1993) for a 70 kg body weight person are: V_p = 2.6 L, V_{lymph} = 5.2 L, L = 2.9 L/day, ISF = 15.6 L, and K_p was set to 0.8 in this case (Wiig et al., 1994; Wiig and Tenstad, 2001). C_p (0) = 1000 nM was selected within the plasma concentration ranges of many mAbs at their therapeutic doses, which is equivalent to peak concentrations of antibody in a 70 kg man after given about 5 mg/kg dose of antibody.

Within the "target tissue" compartment, target-mediated drug disposition (TMDD) component was defined for the binding kinetics between biologics and soluble TNF-α. The differential equations are:

$$\frac{dA}{dt} = C_p \cdot \frac{L_T}{V_T} \cdot (1 - \sigma_V) - A \cdot \frac{L_T}{V_T} \cdot (1 - \sigma_L) - k_{on} \cdot A \cdot Tar + k_{off} \cdot ATar \quad (5)$$

$$\frac{dTar}{dt} = k_{syn} - k_{on} \cdot A \cdot Tar + k_{off} \cdot ATar - k_{deg} \cdot Tar \quad (6)$$

$$\frac{dATar}{dt} = k_{on} \cdot A \cdot Tar - k_{off} \cdot ATar - ATar \cdot \frac{L_T}{V_T} \cdot (1 - \sigma_L) \quad (7)$$

where *A*, *Tar*, and *ATar* are the concentrations for antibody, free-target, and antibody-target complex. Parameters k_{on} and k_{off} are association and dissociation rate constants, k_{syn} and k_{deg} represent target biosynthesis and degradation rates. The *Tar* (0) is defined as target baseline, = k_{syn} / k_{deg}. All Initial Conditions = 0 except *Tar* as 100%. The tissue ISF turnover rate was derived from the equation: $\text{ISF turnover} = L_T/V_T$, where L_T is lymph flow and V_T is ISF volume for a target tissue. The values for L_T and V_T are

JPET Fast Forward. Published on July 12, 2018 as DOI: 10.1124/jpet.118.250134
This article has not been copyedited and formatted. The final version may differ from this version.

assumed as 2% of system lymph flow and 2% of total ISF volume, respectively. All system parameters employed are listed in **Table 1**.With the binding parameters of etanercept, we simulated a range of tissue ISF turnover 0.001 to 100 h^{-1}, which roughly represented the range of ISF turnover in human tissues. The influence of tissue ISF turnover on concentrations versus time profiles of antibody, free target, and antibody-target complex in target tissues were simulated.

Influence of tissue ISF turnover rate on TNF-α suppression

The binding kinetic parameters to human soluble TNF-α were obtained from the literature (Kim et al., 2007; Song et al., 2008), where k_{on} ($\times 10^5\, M^{-1}\cdot s^{-1}$) were 2.59, 0.57 and 1.33, k_{off} ($\times 10^{-4} s^{-1}$) were 13.1, 1.1 and 0.73 for etanercept, infliximab, and adalimumab, respectively. All target binding parameters were summarized in **Table 2**.

The area under target concentrations (*Tar(0)* - *Tar*) versus time curves (ΔAUC) for the three TNF-α antagonists were simulated with a range of ISF turnover rates, which covered the ranges for the colon (re CD) and joint synovium (re RA). As the three biologics have different pharmacokinetics characteristics, degrees of tissue distribution, and approved dosing regimens, it is difficult to accurately predict their target site concentration vs time profiles. Previous PK studies suggested that the three biologics may have similar therapeutic concentrations at their maintenance doses (Tracey et al., 2008). Herein we assumed average antibody PK and tissue distribution kinetics for three biologics (**Table 1**). This approximation allowed us to specifically evaluate the influence of tissue fluid turnover rate and binding kinetic constants on target suppression. The role of tissue ISF turnover on TNF-α suppression was compared among the three biologics.

The TNF-α suppressive effect in two target-associated tissues, joint synovium and colon, was particularly compared.

Interrelationships between tissue fluid turnover and target-binding constants

For a dynamic range of tissue ISF turnover rates (0.001 to 100 h^{-1}), we simulated the influence of increasing k_{on} or decreasing k_{off}, two strategies that could enhance target binding affinity and potentially improve drug efficacy. The impact of binding constants (k_{on} or k_{off}) on tissue accumulation of drug-target complexes was also simulated for a dynamic range of ISF turnover rates.

Survey of licensed biologics

In development of therapeutic antibodies, once a viable target is identified, a next step is to decide at which degree of binding affinity the antibody could achieve a substantial target inhibition. To better understand the relationships between target binding affinity and the ISF turnover rates, we surveyed 27 antibodies that have been approved with soluble targets for many types of diseases. The ISF turnover rates of disease-associated tissues were calculated from the equation L_T / ISF_T, where L_T and ISF_T were lymph flow and ISF volume for specific tissues associated with drug indications collected from the literature (Bauer et al., 1933; Brown et al., 1991; Renkin and Wiig, 1994; Levick, 1998; Shah and Betts, 2012). The biologics adalimumab, belimumab, canakinumab and infliximab, which have indications associated with multiple indications or tissues, were plotted separately for each indication-corresponding tissue. The ISF turnover rate of tumor is normally low considering the collapsed lymphatic system, which was thus set at 0.0001 h^{-1}. The values of average binding affinity for each antibody and the ISF turnover

JPET Fast Forward. Published on July 12, 2018 as DOI: 10.1124/jpet.118.250134
This article has not been copyedited and formatted. The final version may differ from this version.

rates of their target-associated tissues were listed in **Table 2**. The parameter K_a was used (reciprocal of K_d and calculated as k_{on}/k_{off}) to reflect the binding affinity. Besides, target turnover values for each target in Table 2 are listed in Supplemental Table S1.

Simulation and Statistical Analysis

Model simulations were performed using Berkeley Madonna (version 8.3.18; Berkeley Madonna Inc., University of California, Berkeley, CA). All the graphs and statistical analysis were performed using GraphPad Prism 6 software (San Diego, CA, USA). The values on the plots are expressed as mean ± SD.

JPET Fast Forward. Published on July 12, 2018 as DOI: 10.1124/jpet.118.250134
This article has not been copyedited and formatted. The final version may differ from this version.

Results

Influence of tissue ISF turnover on target binding kinetics

In order to evaluate the influence of tissue ISF turnover rate on antibody-target binding kinetics, tissue concentration vs time profiles of antibody, free-target and antibody-target binding complex for different ISF turnover rates from 0.001 to 100 h^{-1} were simulated (**Fig. 2**). When the ISF turnover rate decreases from 100 to 0.001 h^{-1}, the amount of antibody that distributes into the target tissues becomes restricted, as lymphatic convection primarily determines antibody access into disease tissues (**Fig. 2A**). The distribution rate also becomes slower with the decrease of tissue ISF turnover rate. Tissues with higher ISF turnover rate generally experience stronger target suppression (**Fig. 2B**), which is partly associated with greater antibody concentrations in these tissues (**Fig. 2A**). This is also largely ascribed to increased efficiency in removing antibody-target complexes from these tissues through fast lymphatic flow. Efficient removal of complexes drive target binding kinetics towards complex formation (i.e. association). As shown in **Fig. 2C**, antibody-target complex gradually accumulate with the decrease of ISF turnover rates from 100 - 0.1 h^{-1}. Greater accumulation of drug-target complex would disturb binding equilibrium and drive complex dissociation. Once tissue ISF turnover becomes lower than 0.1 h^{-1}, drug-target complex would start decreasing, as there would be insufficient tissue antibodies for binding to the target.

Influence of tissue ISF turnover rates on TNF-α suppression

Compared with infliximab and adalimumab, etanercept is generally regarded as a fast TNF-α binder as it exhibits higher association rate (k_{on} is 2-5-fold higher). In contrast,

JPET Fast Forward. Published on July 12, 2018 as DOI: 10.1124/jpet.118.250134
This article has not been copyedited and formatted. The final version may differ from this version.

infliximab and adalimumab are regarded as stable TNF-α binders, as they both have relatively lower dissociation rates (k_{off} is much slower than that for etanercept). With such distinct binding kinetics, their TNF-α suppressive effects (ΔAUC) in target tissues with changing ISF turnover are shown in **Fig. 3**. For target tissues with relatively slow ISF turnover rate, i.e., on the left side of **Fig. 3**, infliximab and adalimumab show higher TNF-α suppressive effects. Considering that infliximab and adalimumab are both able to form large immune complexes, their effective dissociation rates are even lower than that at 1:1 binding (Scallon et al., 2002). Thus the actual TNF-α suppressive effects for infliximab and adalimumab are expected to be greater than what is shown in **Fig. 3**. Such large immune complexes are seldom observed during etanercept treatment, which would not improve its poor TNF-α suppressive effects at tissue with low fluid turnover. However, along with the increase of tissue ISF turnover, the target suppressive effect of etanercept gradually increases and even surpasses infliximab once tissue ISF turnover rate is > 1 h^{-1}.

Two target tissues, colon (for CD) and joint synovium (for RA) are shown in **Fig. 3** with their reported ISF turnover rates (0.03 ~ 0.06 for colon and 0.15 ~ 1.0 hr^{-1} for JS). In the colon, two stable binders, infliximab and adalimumab, are expected to exhibit much higher target suppression than the fast binder etanercept. In joint synovium, differences in target suppression become smaller, and etanercept may potentially exhibit even greater TNF-α suppression than infliximab. This simulation provides a theoretical explanation for the limited efficacy of etanercept in CD, even though all three biologics showed comparable efficacy in RA at their therapeutic doses.

JPET Fast Forward. Published on July 12, 2018 as DOI: 10.1124/jpet.118.250134
This article has not been copyedited and formatted. The final version may differ from this version.

Interrelationships between tissue fluid turnover and target-binding constants

Optimization of target-binding constants (k_{on} and k_{off}) is a critical step in development of therapeutic antibodies. Here we simulated the potential effect of altering target-binding constants on target suppression for tissues with a dynamic range of ISF turnover rates. As shown in **Fig. 4A**, a gradual increase of k_{on} produces greater target suppression, and there seems to be no capacity-limitation in the simulated range, particularly at tissues with higher ISF turnover. On the other hand, a decrease of k_{off} (**Fig. 4B**), a commonly applied engineering strategy, showed a saturation effect in target suppression. This saturation was particularly apparent for tissues with relatively high ISF turnover rates.

As shown in **Fig. 4C** and **4D**, there is considerable accumulation of drug-target complexes in tissues with relatively slow ISF turnover rates. Stronger binding affinity produces increased accumulation of drug-receptor complex. The increased complex accumulation in tissues with slow ISF turnover rates accounts for their lower target suppression (**Fig. 4A** and **4B**).

Four scenarios defined by target binding affinity and tissue ISF turnover

Considering that tissue ISF turnover rate and target binding affinity both affect target inhibition, herein we have defined four general scenarios based on criteria of: high ISF turnover rate (> 0.0077 hr^{-1}, the system average), high target affinity (> 1 nM^{-1}); high ISF turnover rate, low target affinity (< 1 nM^{-1}); low ISF turnover rate, high target affinity (> 1 nM^{-1}); and low ISF turnover rate, low target affinity (< 1 nM^{-1}).

These scenarios are shown in **Fig. 5A**. For tissues with high ISF turnover rates, fast target binders are favored for target inhibition, as indicated in **Fig. 3** and **Fig. 4A**.

JPET Fast Forward. Published on July 12, 2018 as DOI: 10.1124/jpet.118.250134
This article has not been copyedited and formatted. The final version may differ from this version.

However, there would be a plateau effect at high affinity by lowering k_{off} (**Fig. 4B**). For tissues with relatively low ISF turnover rates, on average, the target suppressive effect would be weaker than for tissues with high ISF turnover rates (**Fig. 2B** and **Fig. 3**), where stable binders are generally favored for therapy. Decreasing k_{off} is expected to be more efficacious than increasing k_{on} to improve target suppression in tissues with low ISF turnover rates. However, both strategies encounter the problem of accumulation of drug-target complexes, which could shift the binding equilibrium towards complex dissociation (**Fig. 4C** and **4D**). In order to effectively enhance target suppression for tissues with slow ISF turnover rates, reduction of complex accumulation should be considered as a therapeutic strategy.

Surveyed licensed biologics

For 27 surveyed biologics, the average target binding affinity and the ISF turnover rates of their corresponding disease tissues were summarized in **Table 2** and in **Fig. 5B**. Based on the scenarios shown in **Fig. 5A**, whole body turnover, calculated from the ratio of total body flow rate and systemic interstitial fluid volume: L / ISF = 0.0077 h^{-1}, is defined as the system average turnover rate and used to demarcate tissues into two scenarios: low-turnover tissues (tumor, bone, and muscle) and high-turnover tissues (colon, skin, joint, lung, kidney, lymph node. and plasma). As shown in **Fig. 5B**, 24 out of 27 (~ 90%) approved biologics are associated with diseases in tissues with high ISF turnover rates. In those tissues with high ISF turnover rates, fast binders with adequate target binding affinities are expected to achieve high target suppression and sufficient therapeutic efficacy. Antibody candidates with fast binding constants thus have a higher

possibility of therapeutic success.

Discussion

Many therapeutic biologics, such as mAbs and infusion proteins, have been developed to neutralize soluble pathogenic ligands in disease-associated tissues (Wang et al., 2016). For those biologics, the magnitude and duration of target neutralization largely predicts their therapeutic efficacy. Optimization of antibody-target binding constants is an essential strategy to improve therapeutic efficacy (Stein and Ramakrishna, 2017; Tiwari et al., 2017). Inspired by the distinct efficacy of three anti-TNF-α biologics (adalimumab, infliximab, etanercept) for CD, we utilized an extended mPBPK model to evaluate the influence of tissue interstitial fluid turnover rates on target suppression for biologics that neutralize soluble targets. The different TNF-α suppression effect of the three biologics were simulated at a dynamic range of tissue fluid turnover rates. Even though these biologics exhibit comparable TNF-α binding affinity at the sub-nM range, adalimumab and infliximab are considered as stable binders because of their relatively lower k_{on} and k_{off} values to soluble TNF-α compared to etanercept. These two stable binders were predicted to have greater target suppression than etanercept in the CD site colon. On the other hand, etanercept is expected to have comparable or a slightly stronger TNF-α suppression than adalimumab and infliximab at the RA site joint synovium. Therefore, the different tissue fluid turnover rates between the colon and joint synovium, may explain why etanercept exhibits limited efficacy in CD.

In this study, an mPBPK model with TMDD in a "target tissue" compartment was developed to demonstrate the importance of tissue fluid turnover rates on the magnitude of target suppression. In the model, tissue degradation of target-antibody complex was assumed negligible and antibody-target complex exhibited similar disposition behavior as

JPET Fast Forward. Published on July 12, 2018 as DOI: 10.1124/jpet.118.250134
This article has not been copyedited and formatted. The final version may differ from this version.

free antibody (Tiwari et al., 2017). In the developed model, the volume of ISF in target tissue was assumed as 2% of total ISF with the lymph flow about 2% of total lymph flow, which makes the amount of antibody that is disposed in the target tissue not a significant factor to system mass balance. For simplicity, the recycled antibody was not considered back into the plasma compartment. In addition, Fc-mediated nonspecific clearance pathway was not separately defined in the model as it has been included as part of the total linear clearance.

For biologics binding to soluble targets, the ISF turnover rate in disease-associated tissues considerably influenced the magnitude and duration of target suppression. Tissue fluid turnover rates were thus systematically assessed as a critical factor for target suppression. As shown in our analysis, tissue fluid turnover rate not only determines tissue concentrations of antibody, but also affects the removal efficiency and accumulation of antibody-target complexes in disease-associated tissue. The latter limits the effect of biologics in suppression of soluble targets. On the other hand, for tissues with relative fast fluid turnover, a ceiling effect was observed when decreasing dissociation rates beyond target tissue fluid turnover rates in seeking to increase binding affinity and further improve therapeutic efficacy. This concept was summarized in **Fig. 5**. For example, in the joint synovium, a tissue with fast fluid turnover, a fast binder (high k_{on}) rather than a stable binder (low k_{off}) is favored for improved target suppression. Target suppression cannot be increased when lowering k_{off} beyond the fluid turnover rate. There is no numerical cutoff of k_{on} and k_{off} values for a given antibody to make it a faster binder or a stable binder as it is dependent on the fluid turnover rates in the target tissues. Fast binders should be antibodies that have high k_{on} to allow antibody and target

JPET Fast Forward. Published on July 12, 2018 as DOI: 10.1124/jpet.118.250134
This article has not been copyedited and formatted. The final version may differ from this version.

sufficiently bind during the fluid turnover process of their target tissues. Stable binders should be antibodies that have low k_{off} to keep the antibody-target complex during tissue fluid turnover. These findings have implications to prioritize strategies for development of biologics for soluble targets in tissues.

Optimization of target binding kinetics to achieve greater binding affinity is the first priority in developing biologics. However, as shown in our analysis, excessive pursuit of high binding affinity is not desirable and even wasteful (Rudnick et al., 2011). Selection of sufficient binding affinity but particularly focusing on appropriate binding constants for a given diseased tissue is a rational approach. In surveying 27 approved biologics with soluble targets, over 90% of the biologics treat diseases associated with tissues having fluid turnover rates higher than the system average. Three exceptions are bevacizumab, romosozumab, and eculizumab. Bevacizumab is an antibody targeting vascular endothelial growth factor (VEGF), a pro-angiogenic cytokine used in treatment of multiple types of cancer (colon cancer, lung cancer, glioblastoma, and renal-cell carcinoma). In solid tumors that are generally believed to have low functional lymphatics, thus bevacizumab-VEGF complexes is expected to accumulate with lesser therapeutic efficacy (Couzin-Frankel and Ogale, 2011; Van Cutsem et al., 2011; Khasraw et al., 2014). For tissues with relatively slow fluid turnover, strategies to increase lymph flow or enhance local degradation of the drug-target complexes might improve target suppression and efficacy.

Our mPBPK model was used to assess the influence of tissue fluid turnover rate on target suppression for biologics bound to soluble antigens. The simulations help explain why etanercept has limited efficacy for CD. For biologics that bind to soluble antigens in

tissues, the interrelationships between target binding constants and tissue fluid turnover rates were also explored showing that accumulation of drug-target complexes in tissues with slow fluid turnover can restrict the magnitude of target suppression. For tissues with high fluid turnover, a plateau effect was suggested for biologics with low target dissociation rates. These findings may help to prioritize strategies in development of therapeutic antibodies for various diseases.

Acknowledgments

We thank Drs. Can Liu and Dongfen Yuan for providing assistance.

Authorship Contributions

Participated in research design: Li, Jusko, and Cao.

Conducted experiments: Li and Cao.

Performed data analysis: Li and Cao.

Wrote or contributed to the writing of the manuscript: Li, Jusko, and Cao.

References

Aaltonen KJ, Virkki LM, Malmivaara A, Konttinen YT, Nordstrom DC and Blom M (2012) Systematic review and meta-analysis of the efficacy and safety of existing tnf blocking agents in treatment of rheumatoid arthritis. *Plos One* **7**.

Amini-Vaughan ZJ, Martinez-Moczygemba M and Huston DP (2012) Therapeutic strategies for harnessing human eosinophils in allergic inflammation, hypereosinophilic disorders, and cancer. *Curr Allergy Asthma Rep* **12**:402-412.

Bang LM and Keating GM (2004) Adalimumab - A review of its use in rheumatoid arthritis. *Biodrugs* **18**:121-139.

Bauer W, Short CL and Bennett GA (1933) The manner of removal of proteins from normal joints. *J Exp Med* **57**:419-433.

Becker F, Potepalov S, Shehzahdi R, Bernas M, Witte M, Abreo F, Traylor J, Orr WA, Tsunoda I and Alexander JS (2015) Downregulation of Foxc2 increased susceptibility to experimental colitis: influence of lymphatic drainage function? *Inflamm Bowel Dis* **21**:1282-1296.

Beerli RR, Bauer M, Fritzer A, Rosen LB, Buser RB, Hanner M, Maudrich M, Nebenfuehr M, Toepfer JA, Mangold S, Bauer A, Holland SM, Browne SK and Meinke A (2014) Mining the human autoantibody repertoire: isolation of potent IL17A-neutralizing monoclonal antibodies from a patient with thymoma. *MAbs* **6**:1608-1620.

Brown TJ, Laurent UB and Fraser JR (1991) Turnover of hyaluronan in synovial joints: elimination of labelled hyaluronan from the knee joint of the rabbit. *Exp Physiol* **76**:125-134.

Cantini F, Niccoli L and Goletti D (2014) Adalimumab, etanercept, infliximab, and the risk of tuberculosis: data from clinical trials, national registries, and postmarketing surveillance. *J Rheumatol Suppl* **91**:47-55.

Cao YG, Balthasar JP and Jusko WJ (2013) Second-generation minimal physiologically-based pharmacokinetic model for monoclonal antibodies. *J Pharmacokinet Phar* **40**:597-607.

Cao YG and Jusko WJ (2014a) Incorporating target-mediated drug disposition in a minimal physiologically-based pharmacokinetic model for monoclonal antibodies. *J Pharmacokinet Phar* **41**:375-387.

Cao YG and Jusko WJ (2014b) Survey of monoclonal antibody disposition in man utilizing a minimal physiologically-based pharmacokinetic model. *J Pharmacokinet Phar* **41**:571-580.

Carter PJ (2006) Potent antibody therapeutics by design. *Nat Rev Immunol* **6**:343-357.

Chen X, DuBois DC, Almon RR and Jusko WJ (2017) Interrelationships between infliximab and recombinant tumor necrosis factor-alpha in plasma using minimal physiologically based pharmacokinetic models. *Drug Metab Dispos* **45**:790-797.

Chen X, Jiang XL, Jusko WJ, Zhou HH and Wang WR (2016) Minimal physiologically-based pharmacokinetic (mPBPK) model for a monoclonal antibody against interleukin-6 in mice with collagen-induced arthritis. *J Pharmacokinet Phar* **43**:291-304.

Chouinard L, Felx M, Mellal N, Varela A, Mann P, Jolette J, Samadfam R, Smith SY, Locher K, Buntich S, Ominsky MS, Pyrah I and Boyce RW (2016) Carcinogenicity risk assessment of romosozumab: A review of scientific

weight-of-evidence and findings in a rat lifetime pharmacology study. *Regul Toxicol Pharmacol* **81**:212-222.

Couzin-Frankel J and Ogale Y (2011) FDA. Once on 'fast track,' avastin now derailed. *Science* **333**:143-144.

Davies B and Morris T (1993) Physiological-parameters in laboratory-animals and humans. *Pharmaceut Res* **10**:1093-1095.

De Luca C and Trifonova A (2017) Patent disclosure requirements for therapeutic antibody patents. *Expert Opin Ther Pat* **27**:867-875.

Deisseroth A, Ko CW, Nie L, Zirkelbach JF, Zhao L, Bullock J, Mehrotra N, Del Valle P, Saber H, Sheth C, Gehrke B, Justice R, Farrell A and Pazdur R (2015) FDA approval: siltuximab for the treatment of patients with multicentric Castleman disease. *Clin Cancer Res* **21**:950-954.

Eigenmann MJ, Karlsen TV, Krippendorff BF, Tenstad O, Fronton L, Otteneder MB and Wiig H (2017) Interstitial IgG antibody pharmacokinetics assessed by combined in vivo- and physiologically-based pharmacokinetic modelling approaches. *J Physiol* **595**:7311-7330.

Eikelboom JW, Quinlan DJ, van Ryn J and Weitz JI (2015) Idarucizumab: The antidote for reversal of dabigatran. *Circulation* 132:2412-2422.

Fallahi-Sichani M, Flynn JL, Linderman JJ and Kirschner DE (2012) Differential risk of tuberculosis reactivation among anti-TNF therapies is due to drug binding kinetics and permeability. *J Immunol* **188**:3169-3178.

Feldmann M, Brennan FM and Maini RN (1996) Role of cytokines in rheumatoid arthritis. *Annu Rev Immunol* **14**:397-440.

Garg A and Balthasar JP (2007) Physiologically-based pharmacokinetic (PBPK) model to predict IgG tissue kinetics in wild-type and FcRn-knockout mice. *J Pharmacokinet Phar* **34**:687-709.

Garrison L and McDonnell ND (1999) Etanercept: therapeutic use in patients with rheumatoid arthritis. *Ann Rheum Dis* **58**:65-69.

Gibbs JP, Doshi S, Kuchimanchi M, Grover A, Emery MG, Dodds MG, Gibbs MA, Somaratne R, Wasserman SM and Blom D (2017) Impact of Target-Mediated Elimination on the Dose and Regimen of Evolocumab, a Human Monoclonal Antibody Against Proprotein Convertase Subtilisin/Kexin Type 9 (PCSK9). *J Clin Pharmacol* **57**:616-626.

Greig SL (2016) Brodalumab: first global approval. *Drugs* **76**:1403-1412.

Guo R, Zhou Q, Proulx ST, Wood R, Ji RC, Ritchlin CT, Pytowski B, Zhu Z, Wang YJ, Schwarz EM and Xing L (2009) Inhibition of lymphangiogenesis and lymphatic drainage via vascular endothelial growth factor receptor 3 blockade increases the severity of inflammation in a mouse model of chronic inflammatory arthritis. *Arthritis Rheum* **60**:2666-2676.

Hart TK, Cook RM, Zia-Amirhosseini P, Minthorn E, Sellers TS, Maleeff BE, Eustis S, Schwartz LW, Tsui P, Appelbaum ER, Martin EC, Bugelski PJ and Herzyk DJ (2001) Preclinical efficacy and safety of mepolizumab (SB-240563), a humanized monoclonal antibody to IL-5, in cynomolgus monkeys. *J Allergy Clin Immunol* **108**:250-257.

Hernandez LD, Racine F, Xiao L, DiNunzio E, Hairston N, Sheth PR, Murgolo NJ and Therien AG (2015) Broad coverage of genetically diverse strains of Clostridium

difficile by actoxumab and bezlotoxumab predicted by in vitro neutralization and epitope modeling. *Antimicrob Agents Chemother* **59**:1052-1060.

Horiuchi T, Mitoma H, Harashima S, Tsukamoto H and Shimoda T (2010) Transmembrane TNF-alpha: structure, function and interaction with anti-TNF agents. *Rheumatology (Oxford)* **49**:1215-1228.

Khasraw M, Ameratunga MS, Grant R, Wheeler H and Pavlakis N (2014) Antiangiogenic therapy for high-grade glioma. *Cochrane Database Syst Rev*:CD008218.

Kim MS, Lee SH, Song MY, Yoo TH, Lee BK and Kim YS (2007) Comparative analyses of complex formation and binding sites between human tumor necrosis factor-alpha and its three antagonists elucidate their different neutralizing mechanisms. *J Mol Biol* **374**:1374-1388.

Levick JR (1998) A method for estimating macromolecular reflection by human synovium, using measurements of intra-articular half lives. *Ann Rheum Dis* **57**:339-344.

Lindena J, Kupper W and Trautschold I (1986) Catalytic enzyme activity concentration in thoracic duct, liver, and intestinal lymph of the dog, the rabbit, the rat and the mouse. Approach to a quantitative diagnostic enzymology, II. Communication. *J Clin Chem Clin Biochem* **24**:19-33.

Liu L, Lu J, Allan BW, Tang Y, Tetreault J, Chow CK, Barmettler B, Nelson J, Bina H, Huang L, Wroblewski VJ and Kikly K (2016) Generation and characterization of ixekizumab, a humanized monoclonal antibody that neutralizes interleukin-17A. *J Inflamm Res* **9**:39-50.

Markham A and Lamb HM (2000) Infliximab - A review of its use in the management of

rheumatoid arthritis. *Drugs* **59**:1341-1359.

Mazumdar S (2009) Raxibacumab. *MAbs* **1**:531-538.

Nagy CF, Mondick J, Serbina N, Casey LS, Carpenter SE, French J and Guttendorf R (2017) Animal-to-human dose translation of obiltoxaximab for treatment of inhalational anthrax under the US FDA animal rule. *Clin Transl Sci* **10**:12-19.

Olesen CM, Coskun M, Peyrin-Biroulet L and Nielsen OH (2016) Mechanisms behind efficacy of tumor necrosis factor inhibitors in inflammatory bowel diseases. *Pharmacol Therapeut* **159**:110-119.

Patel AM and Moreland LW (2010) Certolizumab pegol: a new biologic targeting rheumatoid arthritis. *Expert Rev Clin Immunol* **6**:855-866.

Pizarro TT and Cominelli F (2007) Cytokine therapy for Crohn's disease: Advances in translational research. *Annu Rev Med* **58**:433-444.

Platania CBM, Di Paola L, Leggio GM, Romano GL, Drago F, Salomone S and Bucolo C (2015) Molecular features of interaction between VEGFA and anti-angiogenic drugs used in retinal diseases: a computational approach. *Front Pharmacol* **6**.

Poirier S and Mayer G (2013) The biology of PCSK9 from the endoplasmic reticulum to lysosomes: new and emerging therapeutics to control low-density lipoprotein cholesterol. *Drug Des Devel Ther* **7**:1135-1148.

Renkin EM and Wiig H (1994) Limits to steady-state lymph flow rates derived from plasma-to-tissue uptake measurements. *Microvasc Res* **47**:318-328.

Rondeau JM, Ramage P, Zurini M and Gram H (2015) The molecular mode of action and species specificity of canakinumab, a human monoclonal antibody neutralizing IL-1beta. *MAbs* **7**:1151-1160.

Rother RP, Rollins SA, Mojcik CF, Brodsky RA and Bell L (2007) Discovery and development of the complement inhibitor eculizumab for the treatment of paroxysmal nocturnal hemoglobinuria. *Nat Biotechnol* **25**:1256-1264.

Rudnick SI, Lou J, Shaller CC, Tang Y, Klein-Szanto AJ, Weiner LM, Marks JD and Adams GP (2011) Influence of affinity and antigen internalization on the uptake and penetration of Anti-HER2 antibodies in solid tumors. *Cancer Res* **71**:2250-2259.

Scallon B, Cai A, Solowski N, Rosenberg A, Song XY, Shealy D and Wagner C (2002) Binding and functional comparisons of two types of tumor necrosis factor antagonists. *J Pharmacol Exp Ther* **301**:418-426.

Shah DK and Betts AM (2012) Towards a platform PBPK model to characterize the plasma and tissue disposition of monoclonal antibodies in preclinical species and human. *J Pharmacokinet Phar* **39**:67-86.

Shealy DJ, Cai A, Staquet K, Baker A, Lacy ER, Johns L, Vafa O, Gunn G, 3rd, Tam S, Sague S, Wang D, Brigham-Burke M, Dalmonte P, Emmell E, Pikounis B, Bugelski PJ, Zhou H, Scallon BJ and Giles-Komar J (2010) Characterization of golimumab, a human monoclonal antibody specific for human tumor necrosis factor alpha. *MAbs* **2**:428-439.

Song MY, Park SK, Kim CS, Yoo TH, Kim B, Kim MS, Kim YS, Kwag WJ, Lee BK and Baek K (2008) Characterization of a novel anti-human TNF-alpha murine monoclonal antibody with high binding affinity and neutralizing activity. *Exp Mol Med* **40**:35-42.

Stein AM and Ramakrishna R (2017) AFIR: A dimensionless potency metric for

characterizing the activity of monoclonal antibodies. *CPT Pharmacometrics Syst Pharmacol* **6**:258-266.

Tiwari A, Abraham AK, Harrold JM, Zutshi A and Singh P (2017) Optimal affinity of a monoclonal antibody: guiding principles using mechanistic modeling. *AAPS J* **19**:510-519.

Tracey D, Klareskog L, Sasso EH, Salfeld JG and Tak PP (2008) Tumor necrosis factor antagonist mechanisms of action: a comprehensive review. *Pharmacol Ther* **117**:244-279.

Van Cutsem E, Lambrechts D, Prenen H, Jain RK and Carmeliet P (2011) Lessons from the adjuvant bevacizumab trial on colon cancer: what next? *J Clin Oncol* **29**:1-4.

van Schouwenburg PA, Rispens T and Wolbink GJ (2013) Immunogenicity of anti-TNF biologic therapies for rheumatoid arthritis. *Nat Rev Rheumatol* **9**:164-172.

Wang B, Wu CY, Jin D, Vicini P and Roskos L (2018) Model-based discovery and development of biopharmaceuticals: a case study of mavrilimumab. *CPT Pharmacometrics Syst Pharmacol* **7**:5-15.

Wang W, McIntosh TS, Jiang X, Doddareddy R, Dell EC and Zhou H (2016) Deciphering the in vivo performance of a monoclonal antibody to neutralize its soluble target at the site of action in a mouse collagen-induced arthritis model. *Pharm Res* **33**:1040-1049.

Wang W, Wang EQ and Balthasar JP (2008) Monoclonal antibody pharmacokinetics and pharmacodynamics. *Clin Pharmacol Ther* **84**:548-558.

Wiig H, Kaysen GA, Albander HA, Decarlo M, Sibley L and Renkin EM (1994) Interstitial exclusion of IgG in rat-tissues estimated by continuous-infusion. *Am J*

Physiol **266**:H212-H219.

Wiig H and Tenstad O (2001) Interstitial exclusion of positively and negatively charged IgG in rat skin and muscle. *Am J Physiol-Heart C* **280**:H1505-H1512.

Zhou, Theil H and FrankPeter (2015) Adme and translational pharmacokinetics / pharmacodynamics of therapeutic proteins. *Gut* **60**:774-779.

Zhou Q, Guo R, Wood R, Boyce BF, Liang Q, Wang YJ, Schwarz EM and Xing L (2011) Vascular endothelial growth factor C attenuates joint damage in chronic inflammatory arthritis by accelerating local lymphatic drainage in mice. *Arthritis Rheum* **63**:2318-2328.

Footnotes

This work was supported by the National Institutes of Health National Institute of General Medical Sciences [Grants R35 GM19661, R01 GM24211].

Figure Legends:

Fig. 1. Second-generation minimal PBPK model extended with target binding kinetics and ISF turnover in target tissues. The plasma compartment (dashed line) on the left is exactly the same compartment as the plasma compartment on the right. This layout of model structure is consistent with that for full PBPK models. Dashed line of recycled antibody in the target tissue compartment indicates that there is no recycled antibody considered back into lymph node compartment as the recycled antibody and antibody-target complex account for only a small fraction of total antibody. Symbols are defined in Table 1 and physiological restrictions are defined in Eq. 1-7.

Fig. 2. Simulated target tissue concentration vs time profiles of free antibody (A), free-target (B), antibody-target binding complex (C) at a dynamic range of tissue interstitial fluid turnover rates from 0.001 to 100 h^{-1}. Tissue interstitial fluid turnover rates greatly influence target binding kinetics. Tissues with high fluid turnover are expected to have higher target suppression, which is partly ascribed to increased distribution of antibody and high efficiency in removal of drug-target complexes.

Fig. 3. Simulated interrelationships between tissue fluid turnover rate and the TNF-α suppressive effects (ΔAUC) by three anti-TNF-α biologics at a dynamic range of tissue interstitial fluid turnover rates. Simulation was performed using the binding constants (see Table 1) of each biologic to soluble TNF-α at their therapeutic doses. For joint (re RA), etanercept shows comparable or slightly higher target suppression than adalimumab and inflixiamb. However, for colon (re CD), etanercept exhibits much less target

suppression than the other two biologics.

Fig. 4. Influence of changing antibody-target binding kinetics (k_{on} and k_{off}) for a dynamic range of tissue interstitial fluid turnover rates on minimum concentrations of free target (A, B) and accumulation of antibody-target complex (C, D). There is a plateau effect by lowering k_{off} to improve binding affinity, particularly for tissues with relatively slow interstitial fluid turnover rates.

Fig. 5. Four scenarios proposed based on the binding affinity (K_a , = k_{on}/k_{off}) and tissue fluid turnover rate. (A) For tissues with low fluid turnover, stable binders are generally favored but high affinity often confers increased accumulation of antibody-target complex; for tissues with high fluid turnover, fast binders are generally favored but lowering k_{off} beyond fluid turnover rate produces a plateau effect. (B) Summary of 27 licensed antibodies that bind to soluble ligands for treatment of various diseases. Of these, 24 were approved for treatment of diseases that are associated with tissues with relatively high fluid turnover.

TABLE 1. Model parameters employed for the extended minimal PBPK model simulations

Parameters	Definitions	Values	Unit	Reference
σ_1	Vascular reflection coefficient for tight tissue	0.95	-	(Cao and Jusko, 2014b)
σ_2	Vascular reflection coefficient for leaky tissue	0.71	-	(Cao and Jusko, 2014b)
σ_L	Lymphatic reflection coefficient	0.20	-	(Garg and Balthasar, 2007)
σ_V	Vascular reflection coefficient for target tissue	0.50	-	(Cao and Jusko, 2014a)
L	Total lymph flow	2.9/24	$L \cdot h^{-1}$	(Lindena et al., 1986)
L_1	Lymph flow for tight tissue	0.0399	$L \cdot h^{-1}$	(Shah and Betts, 2012)
L_2	Lymph flow for leaky tissue	0.081	$L \cdot h^{-1}$	(Shah and Betts, 2012)
CL_p	Systemic clearance	0.01	$L \cdot h^{-1}$	(Cao and Jusko, 2014b)
L_T	Lymph flow for target tissue (2% of total)	0.00242	$L \cdot h^{-1}$	(Davies and Morris, 1993)
V_{tight}	ISF for tight tissue	8.112	L	(Cao and Jusko, 2014a)
V_{leaky}	ISF for leaky tissue	4.368	L	(Cao and Jusko, 2014a)
V_T	ISF for target tissue (2% of total ISF)	0.314	L	(Davies and Morris, 1993)
V_{lymph}	Lymph volume	5.2	L	(Davies and Morris, 1993)

V_p	Plasma volume	2.6	L	(Davies and Morris, 1993)
k_{deg}	Free target degradation rate	4.2	h^{-1}	(Cao and Jusko, 2014a)
k_{syn}	Target biosynthesis rate in target tissue	4.2	$nM \cdot h^{-1}$	(Cao and Jusko, 2014a)

TABLE 2. Properties related to 27 surveyed therapeutic antibodies

Antibodies	Average K_D (nM)	Target	Target tissue	ISF turnover (h^{-1})	Reference[a]
Bevacizumab	1.10	VEGF	Tumor	0.0001	(Carter, 2006)
Romosozumab	0.01	Sclerostin	Bone	0.003	(Chouinard et al., 2016)
Eculizumab	0.12	C5	Muscle	0.007	(Rother et al., 2007)
Belimumab	0.20	BAFF	Whole Body	0.0077	(Zhou et al., 2015)
Ranibizumab	0.046	VEGF	Whole Body		(Platania et al., 2015)
Adalimumab	0.55	TNF-α	Colon		(Song et al., 2008)
Bezlotoxumab	0.75	*Clostridium difficile*	Colon	0.04	(Hernandez et al., 2015)
Infliximab	1.92	TNF-α	Colon		(Kim et al., 2007)
Brodalumab	0.239	IL-17RA	Skin		(Greig, 2016)
Ixekizumab	0.0018	IL-17A	Skin	0.05	(Liu et al., 2016)
Secukinumab	0.166	IL-17A	Skin		(Beerli et al., 2014)
Ustekinumab	0.10	IL-12, IL-23	Skin		(De Luca and Trifonova, 2017)

Adalimumab	0.55	TNF-α	Joint Synovium		(Song et al., 2008)
Canakinumab	0.031	IL-1β	Joint Synovium		(Rondeau et al., 2015)
Certolizumab Pegol	0.09	TNF-α	Joint Synovium		(Patel and Moreland, 2010)
Etanercept	5.10	TNF-α	Joint Synovium	0.15	(Kim et al., 2007)
Golimumab	0.018	TNF-α	Joint Synovium		(Shealy et al., 2010)
Infliximab	1.92	TNF-α	Joint Synovium		(Kim et al., 2007)
Mavrilimumab	0.103	GM-CSF	Joint Synovium		(Wang et al., 2018)
Mepolizumab	0.0042	IL-5	Lung		(Hart et al., 2001)
Obiltoxaximab	0.33	*Bacillus anthracis*	Lung		(Nagy et al., 2017)
Omalizumab	0.17	IgE	Lung	1.21	(Carter, 2006)
Raxibacumab	2.78	Anthrax toxin	Lung		(Mazumdar, 2009)
Reslizumab	0.02	IL-5	Lung		(Amini-Vaughan et al., 2012)
Canakinumab	0.031	IL-1β	Kidney	1.46	(Rondeau et al., 2015)
Siltuximab	0.034	IL-6	Ly. Node	7.91	(Deisseroth et al., 2015)
Abciximab	5.00	GPIIb/IIIa	Plasma		(Carter, 2006)

Alirocumab	0.58	PCSK9	Plasma		(Poirier and Mayer, 2013)
Belimumab	0.2	BAFF	Plasma	58.19	(Zhou et al., 2015)
Evolocumab	0.008	PCSK9	Plasma		(Gibbs et al., 2017)
Idarucizumab	0.002	Dabigatran	Plasma		(Eikelboom et al., 2015)

[a] the source of average K_D values for each antibody.

JPET Fast Forward. Published on July 12, 2018 as DOI: 10.1124/jpet.118.250134
This article has not been copyedited and formatted. The final version may differ from this version.

Fig. 1

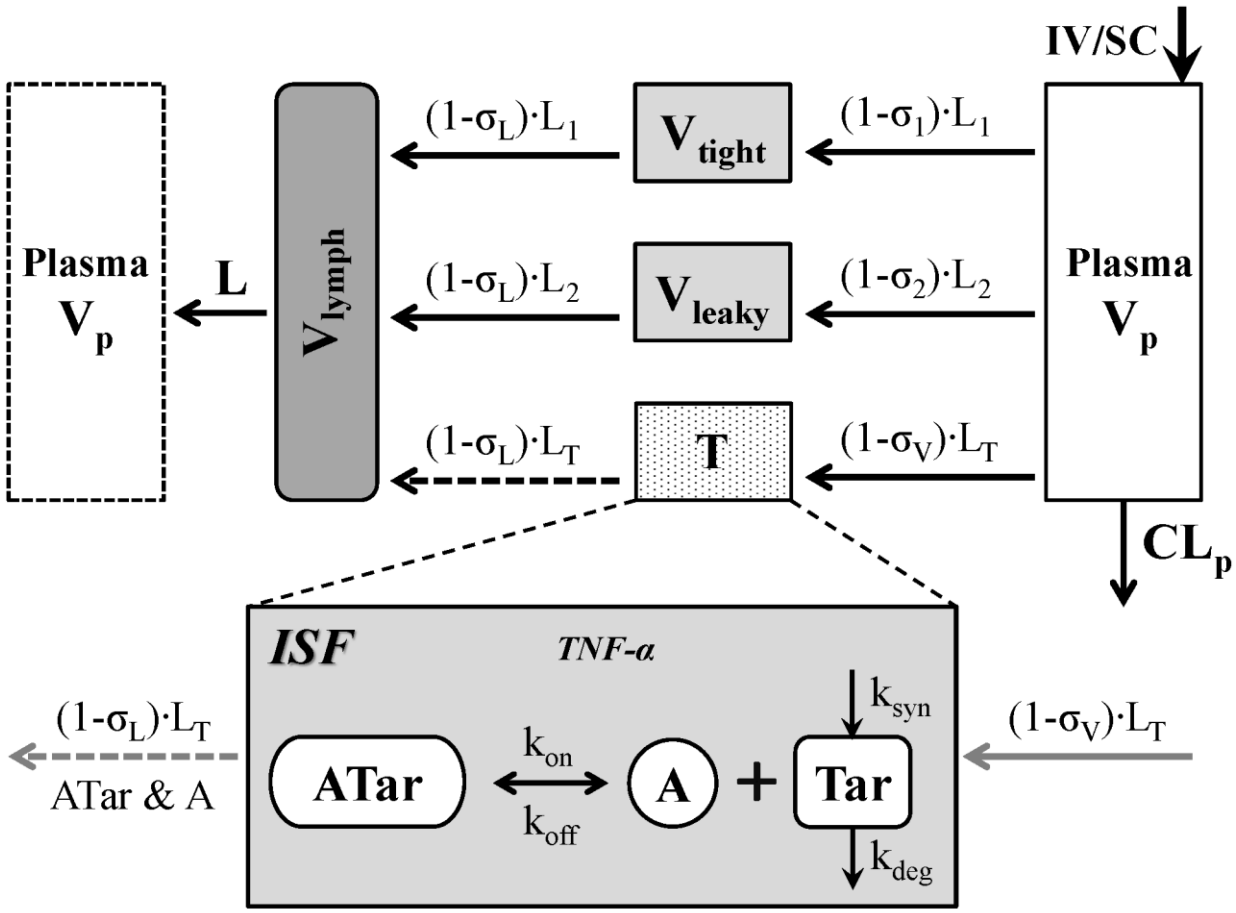

JPET Fast Forward. Published on July 12, 2018 as DOI: 10.1124/jpet.118.250134
This article has not been copyedited and formatted. The final version may differ from this version.

Fig. 2

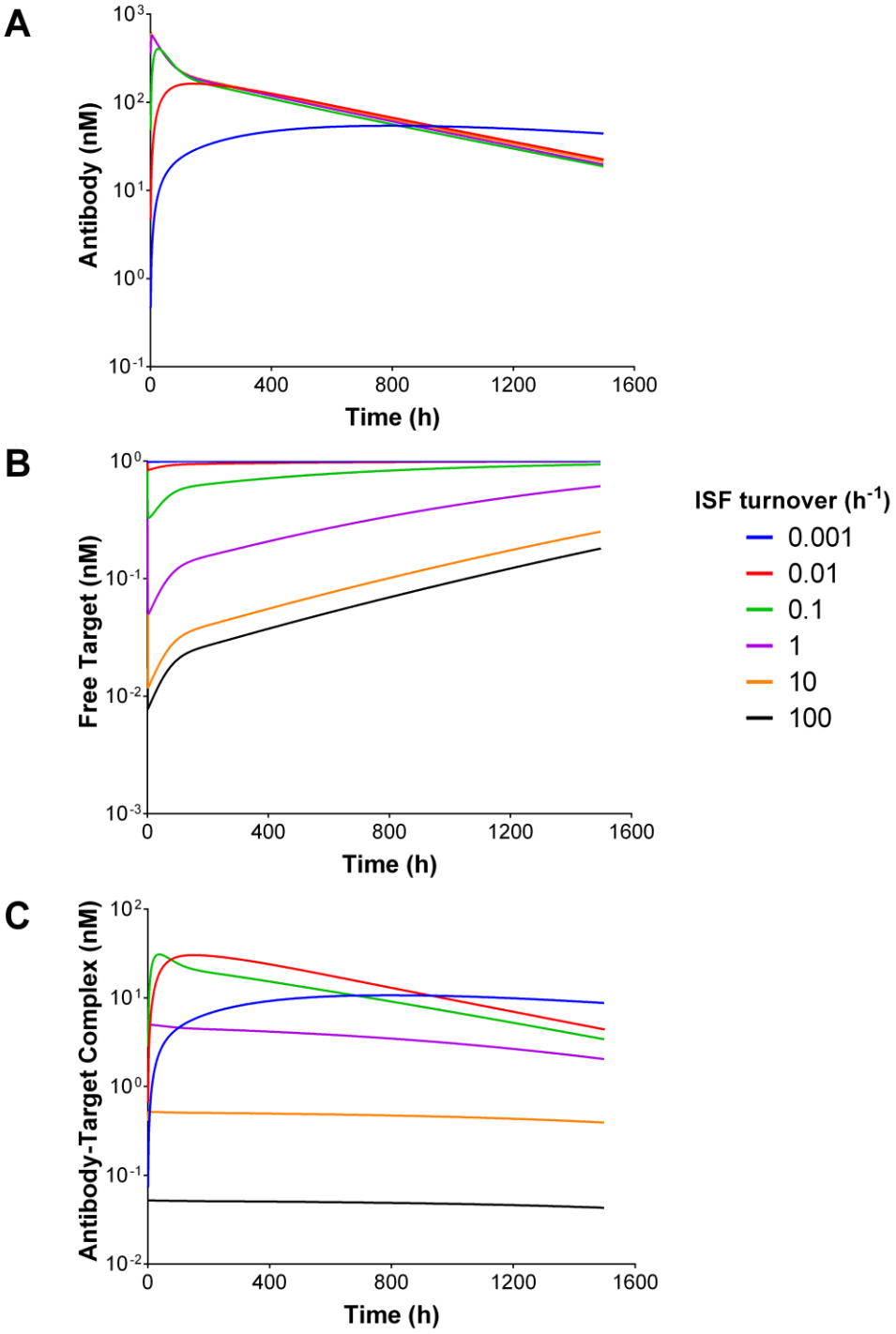

JPET Fast Forward. Published on July 12, 2018 as DOI: 10.1124/jpet.118.250134
This article has not been copyedited and formatted. The final version may differ from this version.

Fig. 3

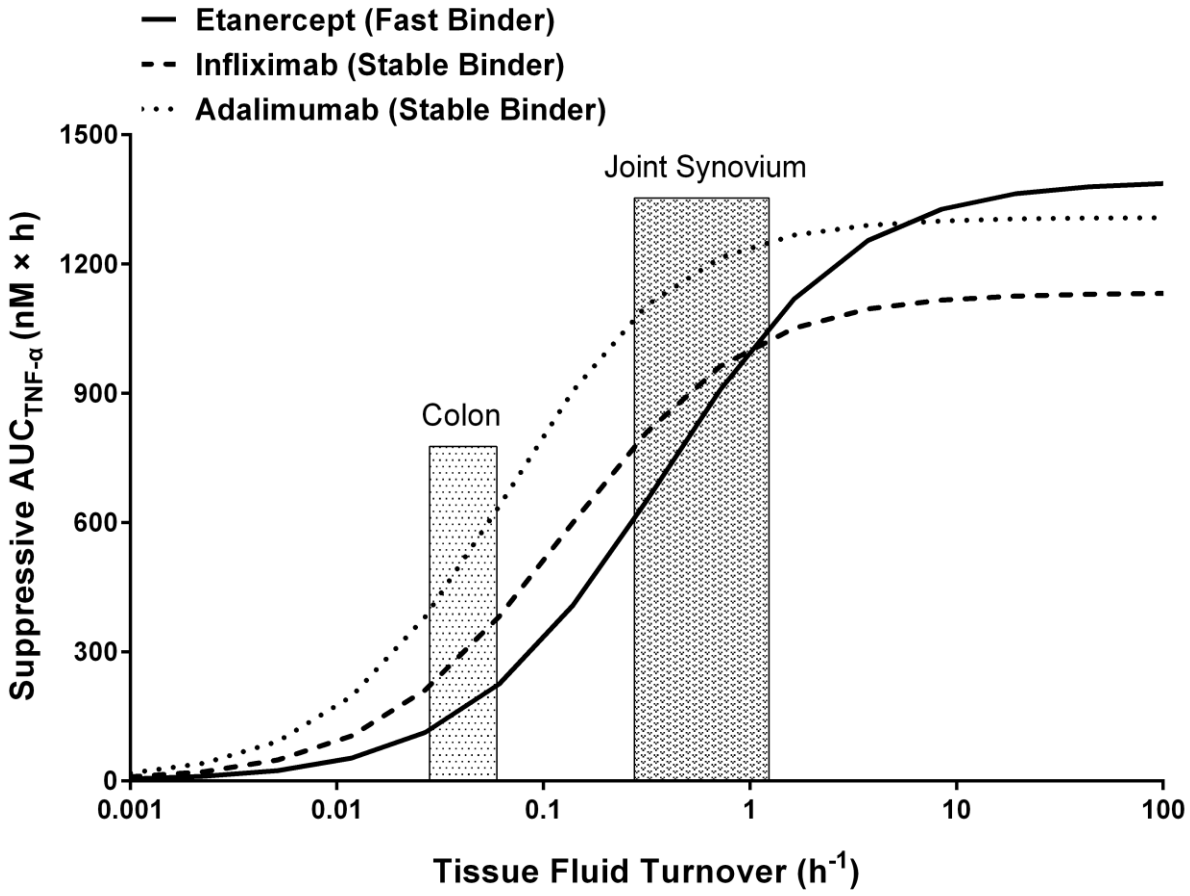

JPET Fast Forward. Published on July 12, 2018 as DOI: 10.1124/jpet.118.250134
This article has not been copyedited and formatted. The final version may differ from this version.

Fig. 4

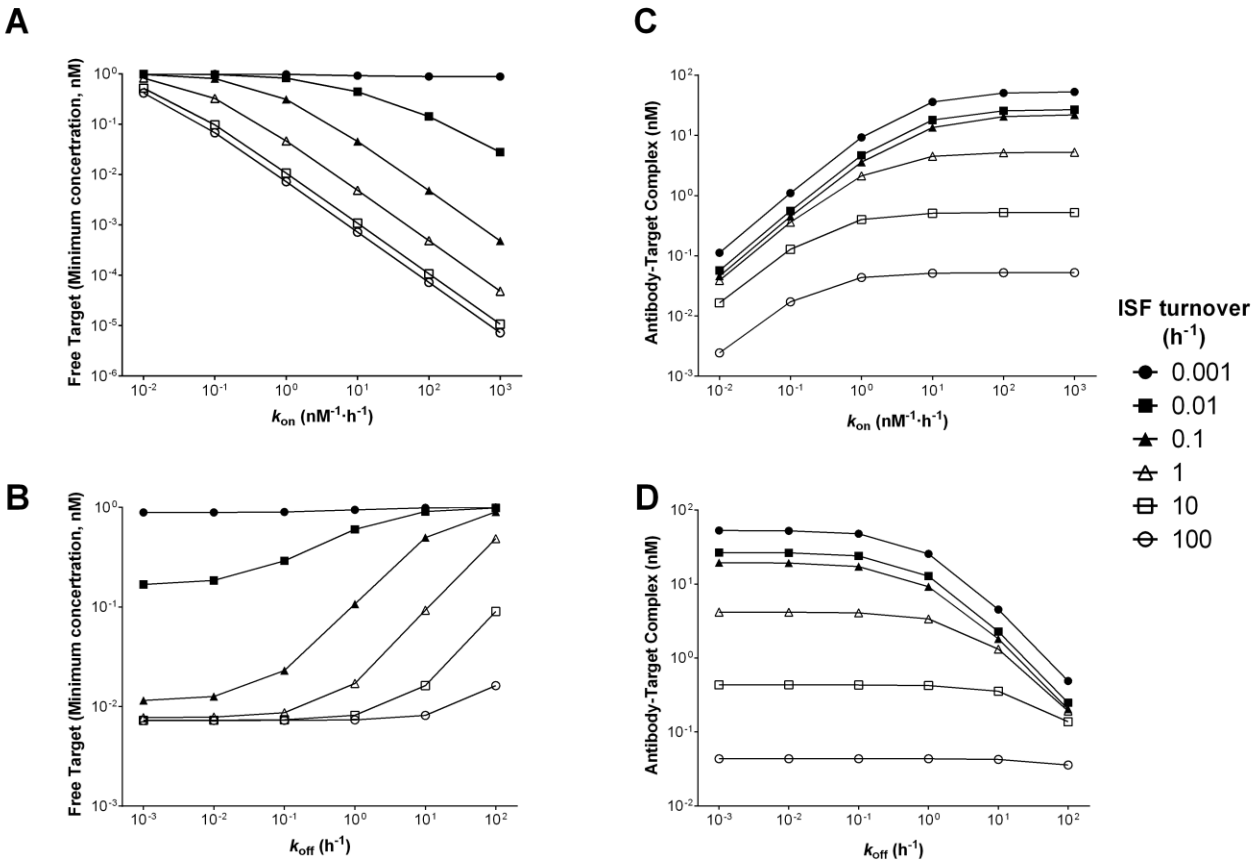

JPET Fast Forward. Published on July 12, 2018 as DOI: 10.1124/jpet.118.250134
This article has not been copyedited and formatted. The final version may differ from this version.

Fig. 5

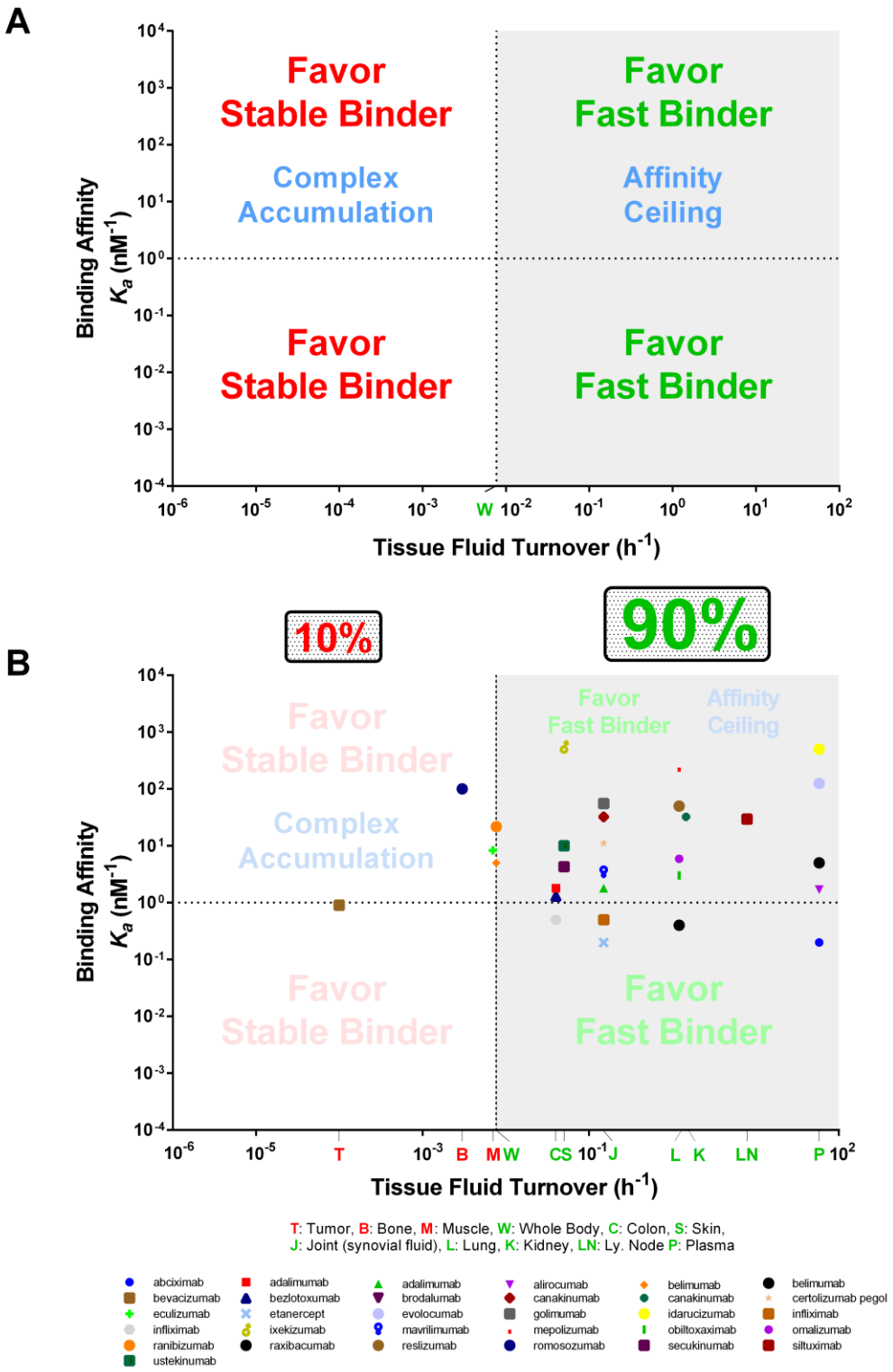

Supplemental Materials-

Journal of Pharmacotherapy and Experimental Therapeutics

Title: Role of interstitial fluid turnover on target suppression by therapeutic biologics using a minimal physiologically-based pharmacokinetic (mPBPK) model

Xiaobing Li, William J. Jusko, and Yanguang Cao

Department of Pharmacy, Shengjing Hospital of China Medical University, Shenyang, China (X.L.); Division of Pharmacotherapy and Experimental Therapeutics, UNC Eshelman School of Pharmacy, University of North Carolina at Chapel Hill, Chapel Hill (X.L., Y.C.); and Department of Pharmaceutical Sciences, School of Pharmacy and Pharmaceutical, Sciences, State University of New York at Buffalo, Buffalo, New York (W.J.J.)

Supplemental Table S1. Target turnover values for each target in Table 2.

Supplemental Table S1.

Target turnover values for each target in Table 2.

Target	Target turnover[a] (h^{-1})	Reference
VEGF	1.22	(Stefanini et al., 2008)
C5	0.033	(Berg et al., 2010)
BAFF	0.594	(Bossen et al., 2011)
TNF-α	4.158	(Waage et al., 1989)
IL-1β	4.158	(Muscat et al., 1995)
GM-CSF	0.16	(Marini et al., 2007)
IL-5	4.158	(Wiesemann et al., 2003)
IgE	0.014	(Hayashi et al., 2007)
Anthrax toxin	0.035	(Kintzer et al., 2010)
IL-6	1.17	(Gerhartz et al., 1994)

[a] Calculated by k_{deg} =0.693/ $t_{1/2}$ where $t_{1/2}$ is the half-life of target in human in hour selected from reference.

Berg CWVD, Horssen PJV, Hofhuis KMA, Aerts PC and Dijk HV (2010) C5 Does Not Play a Major Role in the Immune Response of Mice to SRBC In Vivo. *Scandinavian Journal of Immunology* **33**:621-626.

Bossen C, Tardivel A, Willen L, Fletcher CA, Perroud M, Beermann F, Rolink AG, Scott ML, Mackay F and Schneider P (2011) Mutation of the BAFF furin cleavage site impairs B-cell homeostasis and antibody responses. *Eur J Immunol* **41**:787-797.

Gerhartz C, Dittrich E, Stoyan T, Rose-John S, Yasukawa K, Heinrich PC and Graeve L (1994) Biosynthesis and half-life of the interleukin-6 receptor and its signal transducer gp130. *Eur J Biochem* **223**:265-274.

Hayashi N, Tsukamoto Y, Sallas WM and Lowe PJ (2007) A mechanism-based binding model for the population pharmacokinetics and pharmacodynamics of omalizumab. *Br J Clin Pharmacol* **63**:548-561.

Kintzer AF, Sterling HJ, Tang, II, Williams ER and Krantz BA (2010) Anthrax toxin receptor drives protective antigen oligomerization and stabilizes the heptameric and octameric oligomer by a similar mechanism. *PLoS One* **5**:e13888.

Marini G, Forno G, Kratje R and Etcheverrigaray M (2007) Recombinant human granulocyte-macrophage colony-stimulating factor: effect of glycosylation on pharmacokinetic parameters. *Electronic Journal of Biotechnology* **10**:271-278.

Muscat C, Bertotto A, Ercolani R, Bistoni O, Agea E, Cesarotti M, Fiorucci G, Spinozzi F and Gerli R (1995) Long term treatment of rheumatoid arthritis with high doses of intravenous immunoglobulins: effects on disease activity and serum cytokines. *Ann Rheum Dis* **54**:382-385.

Stefanini MO, Wu FT, Mac Gabhann F and Popel AS (2008) A compartment model of VEGF distribution in blood, healthy and diseased tissues. *BMC Syst Biol* **2**:77.

Waage A, Brandtzaeg P, Halstensen A, Kierulf P and Espevik T (1989) The complex pattern of cytokines in serum from patients with meningococcal septic shock. Association between interleukin 6, interleukin 1, and fatal outcome. *J Exp Med* **169**:333-338.

Wiesemann E, Klatt J, Wenzel C, Heidenreich F and Windhagen A (2003) Correlation of

serum IL-13 and IL-5 levels with clinical response to Glatiramer acetate in patients with multiple sclerosis. *Clin Exp Immunol* **133**:454-460.